WIDER APPLICATION OF JACK-DOWN CONSTRUCTION METHOD



Hajime Yoshida*, Masato Yamada**, Atsushi Hayashi*

For construction of artificial ground in over-track space, we have developed a jack-down construction method that enables cost reduction of approx. 15% from the cost of conventional methods, and suggested a formula to calculate proof strength of socket joints limited to cylindrical columns to be jointed to beams. But angled steel pipe columns are sometimes used for artificial ground to secure distance from the end of the platform or secure indoor floor area.

So, we this time clarified the load carrying system of a socket joint by loading tests using test models with angled columns, and suggested a formula to calculate proof strength for angled columns. We also examined the load carrying system when low-strength filler is applied inside the socket pipe and the effect of repeated loading with an aim of achieving wider application of the jack-down construction method.

Keywords: Socket joint, Jacking down, Angled steel pipe column, Load carrying system, Ultimate strength

1 Introduction

In the construction of artificial ground in over-track space, building temporary sheds and frequent recabling shown in Fig. 1 (a) cause cost increases. Thus, we developed a jack-down construction method that enables cost reduction and work period shortening by omitting temporary sheds and reducing recabling for those sheds (Fig. 1 (b)).

Specifically, artificial ground is built at the height that does not interfere with existing sheds using sockets modularized with column-beam joints of an outer diaphragm type shown in Fig. 2. Then, the ground is jacked down to a specified height after removing existing sheds, and finally it is jointed with columns by filling in the gaps between columns and sockets with mortar or concrete.

We assumed that socket joints are used only for cylindrical steel pipe columns; so, we created a formula to calculate ultimate strength applicable to such columns only. But angled steel pipe columns are sometimes used for artificial ground to secure distance from the end of the platform or to secure indoor floor area. Thus, we carried out loading tests using test models of column-beam joints of artificial ground to clarify the load carrying system of socket joints for angled steel pipe columns; and we studied calculation methods for the ultimate strength of such socket joints.

In order to further clarify the load carrying system of joints, we also carried out loading tests using cylindrical columns filled with low-strength concrete and repeated loading tests using columns applied with peeling-preventive filler. An overview of those tests is as follows.

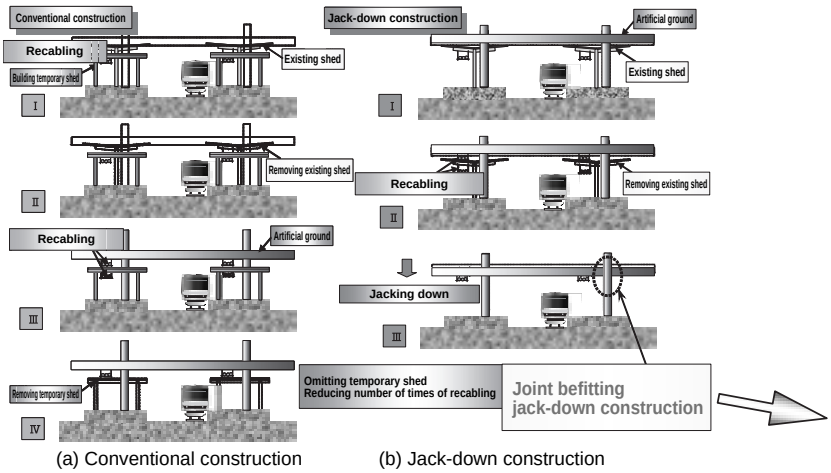

(a) Conventional construction (b) Jack-down construction

Fig.1: Image of Conventional Construction and Jack-down Construction

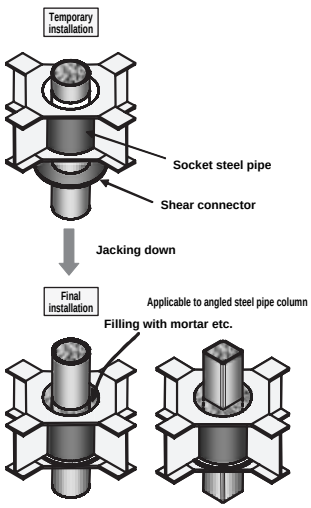

Fig.2: Image of Joint

* Frontier Service Development Laboratory, Research and Development Center of JR East Group
** Tokyo Construction Office (Previously at Frontier Service Development Laboratory)

2 Test of Socket Column-Beam Joint for Angled Steel Pipe Column

2.1 Overview of Test

2.1.1 Shape of Test Model and Specifications

Fig. 3 and Table 1 show the shape and specifications of the test models. They also show the shape and specifications of S-4 and S-5 test models to be explained later and the P-6 test model tested before. Those are T-shape models of column-beam joints. Concrete-filled angled steel pipe columns of the models are inserted into socket steel pipes larger than those columns and joined to the pipes by filling the gaps with mortar. H-shape beams are jointed at the outer diaphragm outside of the socket steel pipes. We defined S-1 as the standard test model. S-2 and S-3 were the test models with different diameters of steel pipes. S-3 was also the test model with concrete-filled angled steel pipe column rotated 45 degrees.

We unified the length of the sides of the angled steel pipes as 1/4 the circumference of the cylindrical steel pipe to make the bearing area of the mortar filler constant. Each test model was flare-welded with 6 mm diameter round steel bars at 50 mm intervals on the circumference as well as on the side of the inside of the socket steel pipes and outside of the column steel pipes to gain higher adhesion of the surfaces of steel pipes and the mortar filler.

In the tests this time, we specified the thickness of the walls of the steel pipe columns and the socket steel pipes to cause destruction of joints without yield of steel pipe columns. Specifically, we used SS400 only for socket steel pipes (SM490 for some test models) and SM490 for other model components. As the filler for steel pipe columns, we used concrete of design standard strength 27 N/mm^2; and as the filler for the gaps between columns and socket steel pipes, we used premixed mortar of design standard strength around 45 N/mm^2 (18 N/mm^2 concrete for S-4 test model). Table 2 shows the yield points of the steel material used and the strength of concrete and mortar used on the test day.

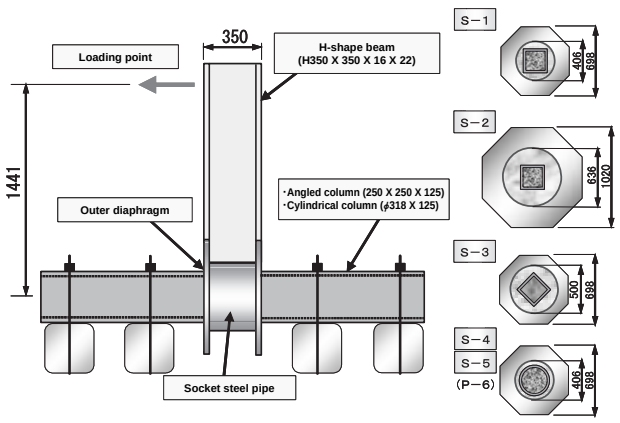

Fig.3: Shape of Test Model

Table.1: Specifications of Test Model

Test model	Steel pipe column d (mm)	Beam (mm)	Socket steel pipe diameter D (mm)	Socket length L (mm)	Socket wall thickness t (mm)	Parameter
S−1	250×250×t25	H350×350×16×22	406	350	6	Angled steel pipe (standard)
S−2	250×250×t25	H350×350×16×22	636	350	6	Angled steel pipe (socket steel pipe diameter)
S−3	250×250×t25	H350×350×16×22	500	350	6	Angled steel pipe (socket steel pipe diameter) Angled steel pipe column rotated 45 degrees
S−4	ϕ318×t25	H350×350×16×22	406	350	6	Cylindrical steel pipe (standard) filled with low-strength concrete
S−5	ϕ318×t25	H350×350×16×22	406	350	6	Cylindrical steel pipe (alternating loading) with prevention of mortar peeling
P−6 (previously tested)	ϕ318×t25	H350×350×16×22	406	350	6	Cylindrical steel pipe (standard)

Table.2: Material Strength

Test model	Yield point (N/mm^2)					Compressive strength (N/mm^2)	
	Socket steel pipe	Column steel pipe	Outer diaphragm	Beam flange	Beam web plate	Column concrete	Mortar filler
S−1	292	369	322	328	371	30.3	73.6
S−2	292	369	322	328	371	31.6	73.2
S−3	394	357	357	357	376	52.6	58.6
S−4	394	357	357	357	376	52.0	15.2
S−5	292	345	357	329	350	39.1	48.4
P−6 (previously tested)	311	321	366	326	330	41.8	51.1

2.1.2 Loading Method

We selected one-side monotonic loading at the point shown in Fig. 3. Loading was carried out until the test model was broken or up to approx. 200 mm, the stroke limit of the jack.

We measured load carrying capacity, displacement of the specified points, and strain of the socket steel pipe, column steel pipe, and outer diaphragm.

2.2 Test Results and Considerations

2.2.1 Destruction Process and Status

First, we will explain the destruction of the standard S-1 test model. Cracking occurred on the side of the mortar filler by the corner of the angled steel pipe, and it developed as loading was repeated. We found gaps between the mortar filler and the socket steel pipe and between the mortar filler and the steel pipe column. Then the strain at a part of the socket steel pipe increased in a 45-degree angle direction to the circumference and reached the yield strain. As the load increased, the crack further developed and the mortar filler came off. Both gaps became larger. The black skin of the outer diaphragm peeled off. Shear deformation of the socket steel pipe developed. Outside deformation of the outer diaphragm also developed. Finally, we suspended the test when the displacement at the loading point reached 250 mm.

S-2 and S-3 test models also broke almost the same way as the S-1 test model, while they differed from S-1 in the position and the direction of the yield strain and damage of each part. Fig. 4 shows the destruction of S-1 test model and Fig. 5 shows the destruction of S-3 test model.

Fig.4: S-1 Test Model

Fig.5: S-3 Test Model

2.2.2 Main Strain Distribution of Socket Steel Pipe

Fig. 6 shows the main strain distribution on the surface of the socket steel pipes. Fig. 6 (a) shows the main strain distribution of S-1 test model at the yield load, and Fig. 6 (b) shows the main strain distribution of the same S-1 test model at the ultimate strength.

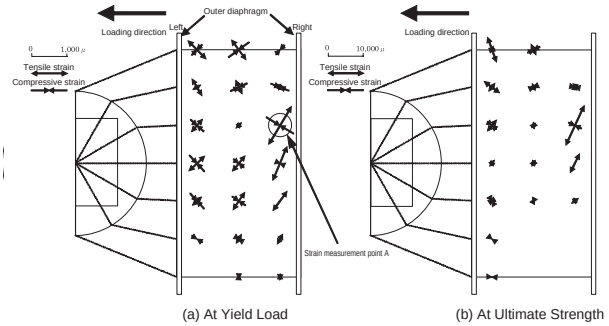

(a) At Yield Load (b) At Ultimate Strength

Fig.6: Main Strain Distribution of Socket Steel Pipe

As for the strain distribution of S-1 at the yield load, Fig. 6 (a) shows that the shear stress (or the diagonal tension) to the socket steel pipe was predominant on the side of the right outer diaphragm (around the strain measurement point A). Since this tendency became more evident as the load increased, we can assume from the diagram that the stress was transmitted to the outer diaphragm via the socket steel pipe. Accordingly, we can assume that the socket steel pipe of S-1 test model worked effectively as the resistance material against the sectional force of the beam because the adhesion between the surface of the socket steel pipe and the mortar filler was strong.

We also found that the main strain distribution of the S-2 test model with larger diameter socket steel pipe was almost the same as the distribution of S-1. As for the S-3 test model with 45-degree rotated column steel pipe, the strain distribution was similar to the distribution of S-1 and S-2, while the diagonal tensile force around the corner was predominant at the ultimate strength. Therefore, we can also assume that the socket steel pipe worked effectively as the resistance material against the sectional force of the beam.

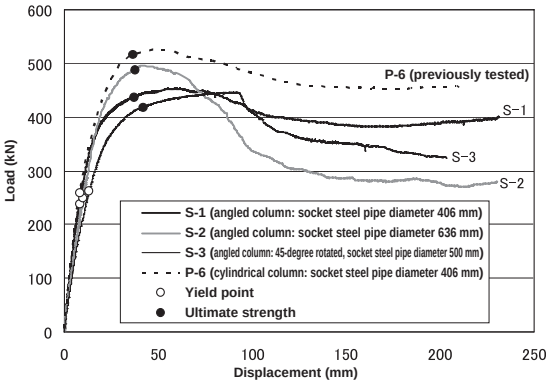

Fig.7: Load-Displacement Relationship

2.2.3 Load-Displacement Relationship

Fig. 7 shows the load-displacement relationship of S-1, S-2 and S-3 test models and P-6 standard test model with cylindrical column (column steel pipe diameter Φ318 × t25mm) tested before. The ● marks in the figure indicate ultimate strength. For convenience, we defined the load at the time when the gradient of the load-displacement relationship tangent dropped to 5% of the initial gradient as the ultimate strength obtained from the test.

Comparing test models with angled columns shown in Fig. 7, we found that the ultimate strength of S-2 was larger than that of S-1. This would be because the outer dimension of the outer diaphragm of S-2 different from that of S-1 had more effect on the ultimate strength of the outer diaphragm. We assume that the proof strength of the outer diaphragm of S-2 dropped after the ultimate loading and that the load decreased more compared with other test models.

The ultimate strength of S-3 test model with 45-degree rotated angled steel pipe column almost matched the ultimate strength of S-1, and there was no deterioration of the ultimate strength affected by column corners. Comparing S-1 and P-7, both standard models in Fig. 7, we found that the ultimate loads of them were different, while the increase of displacement was similar. This would be because the resistance against shear force of the mortar filler of S-1 was lower than that of P-6 with cylindrical column because of the difference in the volume and shape of the mortar filler.

2.3 Calculation of Ultimate Strength of T-Shape Socket Joint

2.3.1 Load Carrying Mechanism for Joints

When we examined main load carrying mechanism for joints in past previous tests with cylindrical steel pipe columns, it was obvious as shown in Fig. 8 that the couple of the bearing force generated between the column steel pipe and the socket steel pipe and the couple of the friction force generated between the column steel pipe and the circle mortar filler resisted the bending moment and the shear force to the joint. So, we suggested Formula (1) to figure out the ultimate strength by solving the equilibrium formula of moments. And considering the different strength shared by the socket steel pipe

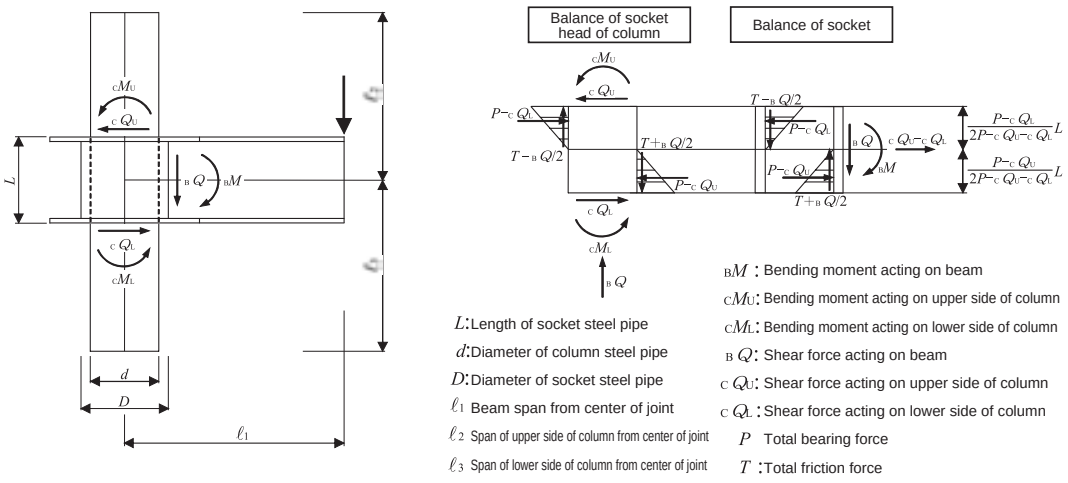

Fig.8: Socket Joint Loading Model

and the outer diaphragm according to shape, we compensated the total bearing force P as shown in Formula (2).

The compensation factor γ derives the correlation among the column steel pipe diameter d, the socket steel pipe diameter D, the socket steel pipe length L, and the socket steel pipe thickness t, and is formulated as Formula (3). Vs, Vc, and Vp represent the resistance against shear force by the socket steel pipe, mortar filler, and outer diaphragm respectively. The component t_s of the formula for X represents the wall thickness of the outer diaphragm.

(Formula for caculating ultimate strength)

$$M_u = \frac{B - \sqrt{B^2 - 4AC}}{2A} \quad \cdots (1)$$

Here

$$A = 16\ell_1^2\left[(\ell_2+\ell_3-L)\left\{12\ell_2\ell_3 - 2\ell_2L - 2\ell_3L - L^2 + 3d(2\ell_3 - L)\tan\phi\right\} + L(2\ell_2 - L)(2\ell_3 - L)\right]$$

$$B = (2\ell_1 - D)\left(4\ell_2\ell_3 - \ell_2L - \ell_3L\right)\left[8P\ell_1(12\ell_2\ell_3 + \ell_2L + \ell_3L - 4L^2) + 6\sqrt{2}d\ell_1\{cdL(2\ell_3 - L) + 2\sqrt{2}P\tan\phi(3\ell_3 + \ell_2 - 2L)\}\right]$$

$$C = (2\ell_1 - D)^2 \cdot (4\ell_2\ell_3 - \ell_2L - \ell_3L)^2 \cdot \left(8LP^2 + 3\sqrt{2}d^2cLP + 12dP^2\tan\phi\right)$$

(Resultant of bearing force)

$$P = (V_s + V_c + V_p)\cdot\gamma \quad \cdots (2)$$

$$\left.\begin{aligned}\gamma &= 0.501X + 0.485\\ X &= (2.97t/D + 1.55t_s/D)(d/D)(L/D)10\end{aligned}\right\} \cdots (3)$$

2.3.2 Calculation of Ultimate Strength of Angled Steel Pipe Column

Our tests using angled steel pipe columns proved that the ultimate strength is lower than that of cylindrical steel pipe columns (Fig. 7). Thus, we replaced the inscribed circle of the angled steel pipe column with a cylindrical steel pipe column, and tried to estimate the ultimate strength from the above-mentioned formula, applying the diameter of the inscribed circle of the angled steel pipe column as d. Replaced with an inscribed circle, the socket steel pipe diameter D apparently becomes larger. So, we tried to adjust the bearing force as shown Formula (4) by multiplying the socket steel pipe diameter D for X in Formula (3) by the compensation factor.

Table 3 and Fig. 9 show a comparison of the values of the ultimate strength of the joints figured out upon the above-mentioned compensation and the actual test result values. The table and the figure show that the figured values could estimate the test values in relatively satisfactory accuracy. Table 3 and Fig. 9 also indicate the figured values and the test values of the cylindrical steel pipe column tested before and S-4 test model to be explained later.

Based on those results, we could clarify the stress transmission system of a socket joint with an angled steel pipe column and expand application of the jack-down construction method.

Table.3: Ultimate Strength Calculated and Actual Test Values

Test model	Test value Puexp (kN)	Calculated value Pucal① (kN)	Puexp /Pucal①	Parameter
P–1	522	517	1.01	Standard
P–2	426	423	1.01	Socket steel pipe diameter
P–3	837	822	1.02	Socket steel pipe length
P–4	686	638	1.08	Socket steel pipe panel thickness
P–5	586	605	0.97	Socket steel pipe diameter
P–6	517	552	0.94	Without fixing plate
P–8	529	503	1.05	Socket steel pipe diameter
S–1	438	429	1.02	Angled steel pipe (standard)
S–2	489	435	1.12	Angled steel pipe (socket steel pipe diameter)
S–3	417	386	1.08	Angled steel pipe rotated 45 degrees (socket diameter)
S–4	408	425	0.96	Low-strength concrete
P–11	514	528	0.97	Without outer diaphragm
P–12	563	544	1.03	Outer diaphragm panel thickness
P–13	488	520	0.94	Outer diaphragm height

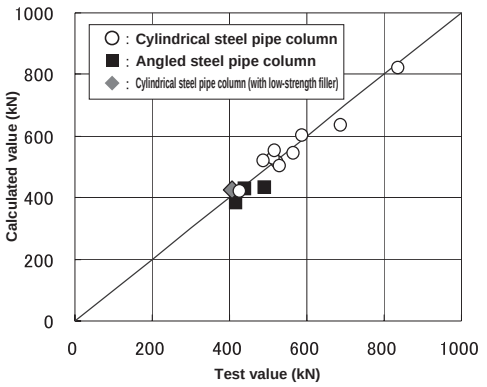

Fig.9: Comparison of Ultimate Strength Calculated and Actual Test Values

3 Test Using Low-Strength Filler in Socket Steel Pipe

3.1 Overview of Test

Next, we carried out monotonic loading tests using a test model (S-4 test model) of a socket steel pipe filled with low-strength concrete (15.2 N/mm² strength). We selected a standard test model with a cylindrical steel pipe column as shown in Fig. 3 and Table 1. The strength of material is shown in Table 2.

3.2 Test Results and Considerations

3.2.1 Destruction Process and Status

The loading test with the S-4 test model showed a similar process and status of destruction to those of the other test models, but the concrete filler on the compressed side was completely broken around the ultimate strength. Fig. 10 shows the destruction status of the low-strength concrete.

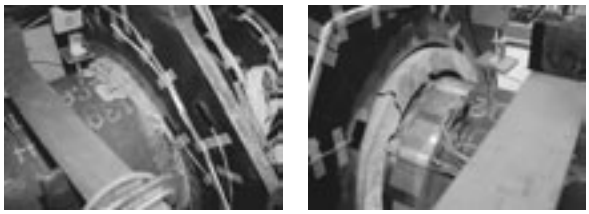

(a) On compressed side at ultimate strength (b) On tensed side at ultimate strength

Fig.10: Destruction Status of Test Model (Low-Strength Filler)

3.2.2 Main Strain Distribution of Socket Steel Pipe

Fig. 11 shows the main strain distribution on the surface of the socket steel pipe at the yield load and the ultimate strength. The figure proved that the S-4 test model had the same strain tendency as that of other test models. The strain in the circumference direction was predominant on some parts of the side of the left outer diaphragm, but we could consider that partial based on the total tendency.

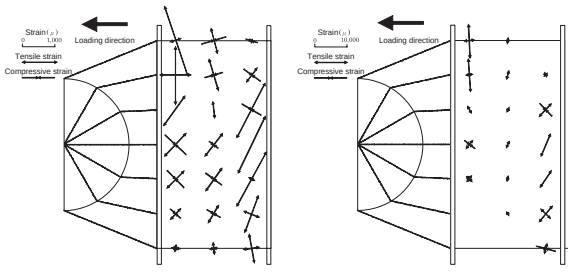

(a) At yield load (b) At ultimate strength

Fig.11: Main Strain Distribution of Socket Steel Pipe (S-4 Test Model)

3.2.3 Load-Displacement Relationship

Fig. 12 shows the load-displacement relationship of the S-4 test model and the P-6 test model used in previous tests. The comparison on the figure confirmed that the ultimate strength dropped by approx. 20%. This could be because the damage to the concrete filler caused deterioration of the resistance against shear force of the concrete filler itself. The figure also indicates evident deterioration of the strength after applying more load than the yield load.

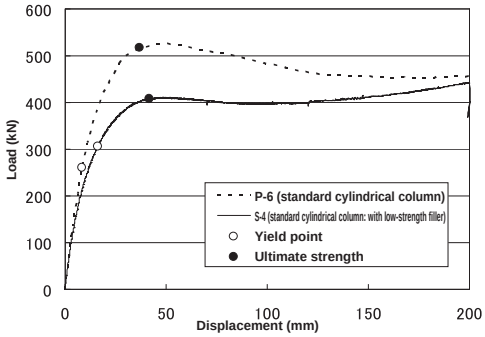

Fig.12: Load-Displacement Relationship

3.3 Calculation of Ultimate Strength with Low-Strength Filler

Table 3 and Fig. 9 show comparisons of the calculation values of the ultimate strength of the cylindrical steel pipe and the actual test result values. Those show that the figured values could estimate the test values in relative satisfactory accuracy. Based on those results, we could consider concrete filler of strength around $\sigma ck = 15$ N/mm² to be useful in the calculation of ultimate strength too.

4 Strength Test of Test Model Loaded Repeatedly

4.1 Overview of Test

The results of the past repeated loading tests (alternating loading tests) of cylindrical steel pipe columns proved that the ultimate strength in alternating loading was about 20% lower than that in monotonic loading. This would be because the resistance against shear force of the mortar filler itself deteriorated due to complete crush by repeated loading; so the resistance function of the outer diaphragm was not so effective as in monotonic loading. Thus, we specified for the ultimate strength in designing a value divided by 1.2 of the value obtained by the ultimate strength calculation formula.

But we can assume that repeated loading does not deteriorate the strength of the mortar filler, when the mortar filler is tied even after complete crushing. So, we carried out alternating loading tests as done previously, binding the mortar filler with silicon material (Fig. 13). The specifications of the test model were specified as a standard cylindrical test model shown in Table 1.

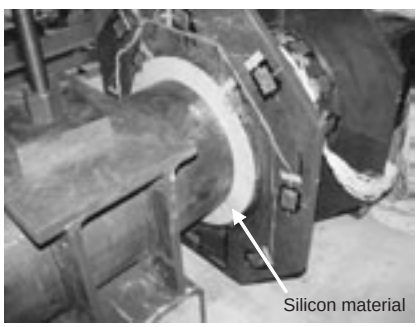

Fig.13: Shape of Test Model

4.2 Destruction Process and Load-Displacement Relationship

Fig. 14 shows the load-displacement relationship of the S-5 test model. It shows a characteristic reverse S-shape history with low energy absorption. The load reached the maximum at the fourth repeated loading, but we found no peeling of silicon at this time at all.

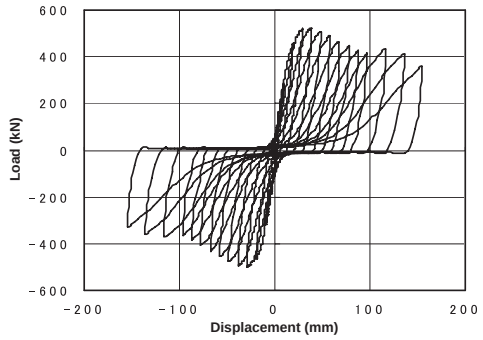

Fig.14: Load-Displacement Relationship

4.3 Comparison with Monotonic Loading

Fig. 15 (a) shows the comparison of the envelope curve of the test model in alternating loading and the load-displacement relationship of the P-6 test model in monotonic loading. Both of the vertical axis and the horizontal axis are made dimensionless with the yield load and the yield displacement. The figure shows that the ultimate strength in monotonic loading and alternating loading are almost equal to each other. Fig. 15 (b) shows the same comparison in the previous tests without binding mortar filler. Comparing Fig. 15 (a) and (b), we clearly found that binding mortar filler prevented the deterioration of the ultimate strength and the deterioration after loading with the ultimate strength was smaller. Therefore, we defined that the value calculated from the ultimate strength formula may be used without lowering adjustment when filler is bound by slabs etc. as in usual buildings.

5 Conclusion

Based on the results of the loading tests this time, we could confirm application of angled steel pipe columns to socket joints, the effect strength of the filler has on the sockets, and easing of conditions for the ultimate strength formula. Accordingly, we could expand application of the jack-down construction method. We obtained structure evaluation of those in March 2006 and formulated the "Socket Joint Design Manual" in July 2006. We are planning to proceed with technical support for application in actual projects.

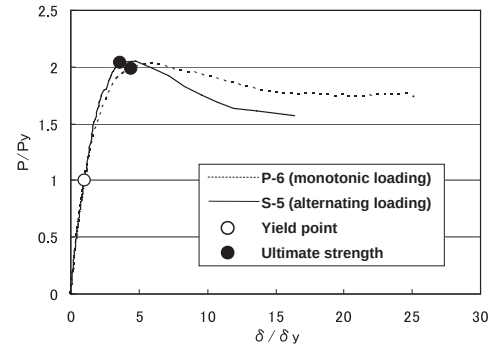

(a) With Biding

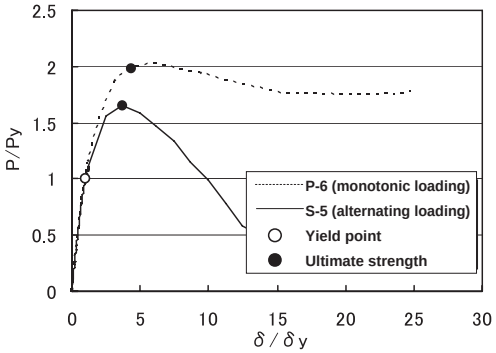

(b) Without Binding

Fig.15: Comparison of Monotonic Loading and Alternating Loading

Reference:

1) Masato Yamada, Atsushi Hayashi, Shin-ichiro Nozawa "Evaluation of Proof Strengths of T-Shape Steel Pipe Socket Column-Beam Joints Filled with Concrete", Theses of Japan Society of Civil Engineers, No. 759/1-67, pp. 293 - 308, April 2004
2) Hisako Kobayashi, Tokiharu Furuya, Masataka Kinoshita "Proof Strength Test of Cross-Shape Socket Column-Beam Joints", Summary of the 24th Kanto Branch Technical Lecture Presentation, V.13, pp. 582 - 583, March 1997
3) Shin-ichiro Nozawa, Masataka Kinoshita, Daisuke Tsukishima, Tadayoshi Ishibashi "Evaluation of Proof Strength of Steel Pipe Socket Joints Filled with Concrete", Theses of Japan Society of Civil Engineers, No. 606/V.41, pp. 31 - 42, November 1998
4) Railway Technical Research Institute "Design Standards of Railway Structures and Commentary: Steel-Concrete Combined Structure", Maruzen Co., Ltd., July 1998
5) Shin-ichiro Nozawa, Masataka Kinoshita, Daisuke Tsukishima, Tadayoshi Ishibashi "Evaluation of Proof Strength of Steel Pipe Socket Joints Filled with Concrete Using Shear Connector", Theses of Japan Society of Civil Engineers, No. 734/V.45, pp. 71 - 89, November 1999